3 Mapping Parametric Confidence Ellipsoids to Nyquist Plane for Linearly Parametrized Transfer Functions*

Xavier Bombois[1], Brian D.O. Anderson[2], and Michel Gevers[1]

[1] Centre for Systems Engineering and Applied Mechanics (CESAME)
Université Catholique de Louvain, B-1348 Louvain-la-Neuve, Belgium
[2] Department of Systems Engineering, Research School of Information Sciences and Engineering, The Australian National University, Canberra ACT 0200, Australia

Abstract. This chapter considers linearly parametrized plants whose parameters are normally distributed and addresses the problem of analyzing the image in the Nyquist plane of a set of these plants defined by a confidence ellipsoid in the parameter space. The image in the Nyquist plane of such set of plants is made up of ellipses at each frequency. However, the connection between different frequencies makes the mapping nontrivial. We show that the probability level linked to this image in the Nyquist plane is larger than that of the confidence region in the parameter space. This is due to the fact that the mapping between the parametric and frequency domain spaces is not bijective.

3.1 Introduction

In many recent works [3,8,12,2], robustness analysis and robust control design have been achieved on frequency domain uncertainty regions containing the true system at a prescribed probability level. This frequency domain uncertainty region represents the frequency responses of parametrized transfer functions [10,9,7]. The parameters of these transfer functions have a Gaussian probability density function that is the result of a prediction error identification experiment. It is therefore important to understand the properties of the mapping from parameter space to Nyquist plane. In this paper, we analyze the particular case of linearly parametrized model structures, which is the case treated e.g. in [8,12,2,7]. For that particular case, we deduce the link between the frequency domain and parametric representations, their differences and the consequences of these differences on the probability level.

* The authors acknowledge the Belgian Programme on Inter-university Poles of Attraction, initiated by the Belgian State, Prime Minister's Office for Science, Technology and Culture. The scientific responsibility rests with its authors. The research reported here has been performed jointly by the three authors. However, the writing has been done by X. Bombois and M. Gevers as a surprise gift to B.D.O. Anderson. Let him share the credit for the ideas, and not be blamed for the text.

For model structures that are linear in the parameter vector θ, the image in the Nyquist plane of a parametric confidence region defined by an ellipsoid U_θ in the parameter space is an uncertainty region made up of ellipses at each frequency in the Nyquist plane. However, the mapping between the parametric and frequency domains is not bijective. We prove that the corresponding uncertainty region in the frequency domain is the image of more parameters θ than those in U_θ and that the probability level linked to the frequency domain confidence region is larger than the one linked to U_θ. We also consider the inverse mapping. We show that, if we consider the ellipses in the Nyquist plane frequency by frequency, they are the image of sets of parameters θ that are different at each frequency.

Chapter outline. In Section 2, we define the set $\mathcal{D}$ that contains the linearly parametrized systems whose parameter vector is constrained to lie in an ellipsoid. In Section 3, we present two theorems that describe the image of an ellipsoid by a nonbijective mapping, as well as the inverse image defined by such mapping. In Section 4, we present the frequency domain set $\mathcal{L}$, image of the set $\mathcal{D}$ in the Nyquist plane. In Section 5, we analyze the inverse image of the set $\mathcal{L}$. In Section 6, we define the probability level linked to $\mathcal{L}$ and give the value of this probability level. In Section 7, we give some comments about the case of model structures that are not linearly parametrized and we finish by an illustration and some conclusions.

3.2 Problem statement

As stated in the introduction, we consider linearly parametrized transfer functions. The case of nonlinearly parametrized transfer functions will be briefly discussed in Section 7. Let us thus consider the following system description:

$$G(z,\theta) = \bar{G}(z) + \Lambda(z)\theta \tag{3.1}$$

with $\theta \in \mathbf{R}^{k\times 1}$ the parameter vector, $\bar{G}(z)$ a known transfer function and $\Lambda(z)$ a known row vector of transfer functions. Let us further assume that θ has a Gaussian probability density function with zero mean[1] and covariance $P_\theta \in \mathbf{R}^{k\times k}$ i.e.

$$\theta \sim \mathcal{N}(0, P_\theta) \tag{3.2}$$

We have therefore:

[1] In the case where $\theta \sim \mathcal{N}(\hat{\theta}, P_\theta)$, one can always write $G(z,\theta) = \bar{G} + \Lambda\hat{\theta} + \Lambda\tilde{\theta} = \bar{G}_{bis} + \Lambda\tilde{\theta}$ with $\tilde{\theta} = \theta - \hat{\theta} \sim \mathcal{N}(0, P_\theta)$

$$\theta^T P_\theta^{-1} \theta \sim \chi^2(k) \tag{3.3}$$

where $\chi^2(k)$ is the chi-square probability density function with k degrees of freedom.

Let us now write the frequency response $g(e^{j\omega},\theta)$ of $G(z,\theta)$ at the frequency ω in the following form:

$$\begin{aligned} g(e^{j\omega},\theta) &\triangleq \begin{pmatrix} Re(G(e^{j\omega},\theta)) \\ Im(G(e^{j\omega},\theta)) \end{pmatrix} \\ &= \overbrace{\begin{pmatrix} Re(\bar{G}(e^{j\omega})) \\ Im(\bar{G}(e^{j\omega})) \end{pmatrix}}^{\bar{g}(e^{j\omega})} + \overbrace{\begin{pmatrix} Re(\Lambda(e^{j\omega})) \\ Im(\Lambda(e^{j\omega})) \end{pmatrix}}^{T(e^{j\omega})} \theta \end{aligned} \tag{3.4}$$

The frequency response vector $g(e^{j\omega},\theta)$ has thus a Gaussian probability density function with mean $\bar{g}(e^{j\omega})$ and covariance $P_g(\omega) = cov((g(e^{j\omega},\theta) - \bar{g}(e^{j\omega}))(g(e^{j\omega},\theta) - \bar{g}(e^{j\omega}))^T) = T(e^{j\omega})P_\theta T(e^{j\omega})^T \in \mathbf{R}^{2\times 2}$. We have thus

$$\begin{aligned} g(e^{j\omega},\theta) &\sim \mathcal{N}(\bar{g}(e^{j\omega}), P_g(\omega)) \\ g(e^{j\omega},\theta)^T P_g(\omega)^{-1} g(e^{j\omega},\theta) &\sim \chi^2(2) \end{aligned} \tag{3.5}$$

The results presented in (3.5) are very common and can e.g. be found in [7]. However, these results do not give a response to some important questions. If we design a confidence ellipsoid in the parameter space using (3.3), is the image of such confidence ellipsoid in the Nyquist plane a confidence region with the same probability level? How can we relate this image with the known probability density function of the frequency response (3.5)? If we design a confidence ellipse at each frequency using (3.5) and define a set by connecting all these ellipses, what is the inverse image of that set in parameter space? In order to answer these questions, we will consider throughout this paper the following confidence ellipsoid in parameter space and the corresponding region in transfer function space. We will choose a probability level of 0.95 for these confidence regions.

Definition 1. Let us consider the parametrized model structure given in (3.1) and the probability density function of the parameter vector θ given in (3.2). The ellipsoid U_θ of size χ:

$$U_\theta = \{\theta \mid \theta^T P_\theta^{-1} \theta < \chi\}, \tag{3.6}$$

with χ such that $Pr(\chi^2(k) < \chi) = 0.95$, is a confidence ellipsoid of probability 0.95 in the parameter space. We define the set $\mathcal{D}$ of transfer functions that correspond to the parameters $\theta \in U_\theta$:

$$\mathcal{D} = \{G(z,\theta) \mid \theta \in U_\theta\} \tag{3.7}$$

The probability level $\alpha(\mathcal{D})$ linked to $\mathcal{D}$ is thus given by $\alpha(\mathcal{D}) \stackrel{\Delta}{=} Pr(G(z,\theta) \in \mathcal{D}) = 0.95$. ■

In the next sections, we describe the image in the Nyquist plane of the uncertainty region $\mathcal{D}$ and we analyze the properties of such image, as well as its inverse image, with respect to the probability level.

3.3 Linear algebra preliminaries

We first present two theorems that describe properties of a mapping T between a real vector y and another real vector x of lower dimension. This mapping has the following expression

$$x = Ty \tag{3.8}$$

where $y \in \mathbf{R}^{k\times 1}$, $x \in \mathbf{R}^{n\times 1}$ $(n < k)$ are real vectors, and $T \in \mathbf{R}^{n\times k}$ is a real matrix of rank n.

Let us first recall a well-known lemma that will be useful to prove the first theorem.

Lemma 1. *Let us consider the partitioned symmetric positive definite matrix* $P \in \mathbf{R}^{k\times k}$*:*

$$P = \begin{pmatrix} P_{11} & P_{12} \\ P_{12}^T & P_{22} \end{pmatrix}$$

with $P_{11} \in \mathbf{R}^{n\times n}$, $P_{12} \in \mathbf{R}^{n\times(k-n)}$ *and* $P_{22} \in \mathbf{R}^{(k-n)\times(k-n)}$. *Let us also consider two real vectors* $x \in \mathbf{R}^{n\times 1}$ *and* $\bar{x} \in \mathbf{R}^{(k-n)\times 1}$ *and an ellipsoid* $U_{x\bar{x}}$ *defined as:*

$$U_{x\bar{x}} = \left\{ \begin{pmatrix} x \\ \bar{x} \end{pmatrix} \mid \begin{pmatrix} x \\ \bar{x} \end{pmatrix}^T P^{-1} \begin{pmatrix} x \\ \bar{x} \end{pmatrix} < 1 \right\}.$$

Then the set U_x

$$U_x \stackrel{\Delta}{=} \{x \mid \begin{pmatrix} x \\ \bar{x} \end{pmatrix} \in U_{x\bar{x}}\} \tag{3.9}$$

is also an ellipsoid given by

$$U_x = \{x \mid x^T P_{11}^{-1} x < 1\} \tag{3.10}$$

Proof. The inverse of the block matrix P can be written (see e.g. [13, page 22])

$$P^{-1} = \begin{pmatrix} K_{11} & K_{12} \\ K_{12}^T & K_{22} \end{pmatrix}$$

where $K_{11} = P_{11}^{-1} + P_{11}^{-1} P_{12} \Delta^{-1} P_{12}^T P_{11}^{-1}$, $K_{12} = -P_{11}^{-1} P_{12} \Delta^{-1}$, $K_{22} = \Delta^{-1}$ and $\Delta = P_{22} - P_{12}^T P_{11}^{-1} P_{12}$.

Using these notations and introducing the vector $z = K_{22}^{-1} K_{12}^T x + \bar{x}$, we have the following equivalences:

$$\begin{aligned} \begin{pmatrix} x \\ \bar{x} \end{pmatrix}^T P^{-1} \begin{pmatrix} x \\ \bar{x} \end{pmatrix} < 1 &\iff x^T (K_{11} - K_{12} K_{22}^{-1} K_{12}^T) x + z^T K_{22} z < 1 \\ &\iff x^T P_{11}^{-1} x + z^T K_{22} z < 1 \end{aligned} \tag{3.11}$$

Using this last expression, we can now write that

i. if $(x^T \ \bar{x}^T)^T \in U_{x\bar{x}}$, then $x^T P_{11}^{-1} x < 1$. Indeed

$$\begin{pmatrix} x \\ \bar{x} \end{pmatrix}^T P^{-1} \begin{pmatrix} x \\ \bar{x} \end{pmatrix} < 1 \Longrightarrow x^T P_{11}^{-1} x < (1 - z^T K_{22} z) < 1$$

ii. if $x^T P_{11}^{-1} x < 1$ then there exists $\bar{x}$ such that $(x^T \ \bar{x}^T)^T \in U_{x\bar{x}}$. Indeed, take as $\bar{x}$, the vector $\bar{x}$ such that $z = 0$ (i.e. $\bar{x} = -K_{22}^{-1} K_{12}^T x$). Then, $\begin{pmatrix} x \\ -K_{22}^{-1} K_{12}^T x \end{pmatrix} \in U_{x\bar{x}}$.

This completes the proof. ∎

Note that U_x is not the intersection of $U_{x\bar{x}}$ with the subspace $\bar{x} = 0$; it is a larger set. Let us now present our two theorems about the mapping T defined in (3.8).

Theorem 1. *Let us consider the mapping T defined in (3.8) and the ellipsoid U_y of size χ in the y-space:*

$$U_y = \{y \mid y^T P_y^{-1} y < \chi\}, \tag{3.12}$$

with $P_y \in \mathrm{R}^{k \times k}$ a positive definite matrix. The image U_x of U_y by the mapping T i.e. $U_x \stackrel{\Delta}{=} \{x \mid x = Ty \text{ with } y \in U_y\}$ is an ellipsoid in the x-space given by

$$U_x = \{x \mid x^T P_x^{-1} x < \chi\}, \tag{3.13}$$

with $P_x = T P_y T^T \in \mathrm{R}^{n \times n}$.

Proof. Let us first complete the mapping T by generating a nonsingular mapping $\tilde{T}$:

$$\begin{pmatrix} x \\ \bar{x} \end{pmatrix} = \overbrace{\begin{pmatrix} T \\ \bar{T} \end{pmatrix}}^{\tilde{T}} y \tag{3.14}$$

such that $\tilde{T} \in \mathbf{R}^{k \times k}$ has rank k. Using $\tilde{T}$, we have that

$$y^T P_y^{-1} y < \alpha \Longleftrightarrow \begin{pmatrix} x \\ \bar{x} \end{pmatrix}^T \overbrace{\tilde{T}^{-T} P_y^{-1} \tilde{T}^{-1}}^{P^{-1}} \begin{pmatrix} x \\ \bar{x} \end{pmatrix} < \chi \tag{3.15}$$

Proving Theorem 1 is thus equivalent to proving that (3.13) is the domain where x is constrained to lie when (3.15) holds. This follows immediately from Lemma 1, noting that if $P = \tilde{T} P_y \tilde{T}^T$, then $P_x = P_{11} = T P_y T^T$. ∎

Theorem 2. *Let us consider the mapping T and the ellipsoids U_y and U_x defined in (3.8), (3.12) and (3.13), respectively. Define the inverse image C_y of U_x using the mapping T as*

$$C_y \stackrel{\Delta}{=} \{y \mid x = Ty \in U_x\}, \tag{3.16}$$

Then C_y is a volume given by

$$C_y = \{y \mid y^T R_C y < \chi\}, \tag{3.17}$$

with $R_C = T^T P_x^{-1} T$, a singular matrix $\in \mathbf{R}^{k \times k}$. Moreover, the volume C_y has the following properties:

- *The matrix R_C defining C_y has rank n i.e. it has $k - n$ zero eigenvalues. The volume C_y has therefore $k - n$ infinite main axes. The directions y_i $(i = 1...k-n)$ of these infinite main axes are the eigenvectors corresponding to the null eigenvalues of R_C. Moreover, these eigenvectors y_i belong to the null space of T i.e. $Ty_i = 0$.*
- *The ellipsoid U_y is included in C_y.*

Proof. We first prove that the inverse image of U_x by the mapping (3.8) is given by (3.17). This follows directly from:

$$x^T P_x^{-1} x < \chi \Longleftrightarrow y^T T^T P_x^{-1} T y < \chi \tag{3.18}$$

The volume C_y is thus the inverse image of U_x since y has to satisfy the right-hand side of (3.18) in order to have x in U_x.

It follows from $R_C = T^T P_x^{-1} T \in \mathbf{R}^{k \times k}$ with T of rank $n < k$ that R_C has $k - n$ null eigenvalues and that the corresponding eigenvectors are in the null-space of the mapping T.

Theorem 1 and the definition (3.16) of C_y show that U_y is included in C_y. Indeed, we know by Theorem 1 that each y in U_y has an image (i.e. Ty) in U_x. Therefore, each y in U_y lies in C_y defined by (3.16). ■

Comments.

- Since the matrix T has rank $n < k$, the mapping (3.8) is not bijective. This explains the fact that the image of U_y by the mapping (3.8) is exactly U_x and that the inverse image of U_x is a larger volume C_y containing U_y.
- In the particular case where $k = 3$ and $n = 2$, U_x is then an ellipse (Theorem 1) and C_y is a cylinder with infinite axis. The axis of the cylinder is in the direction of the eigenvector corresponding to the single null eigenvalue (Theorem 2).

3.4 Image of $\mathcal{D}$ in the Nyquist plane

Theorem 1 tells us that the image of an ellipsoid by a linear mapping into a smaller dimensional space is also an ellipsoid. This theorem will now be used in order to find the frequency domain region (or dynamic region) that is the image of $\mathcal{D}$ in the Nyquist plane. This frequency domain region is defined via a constraint on the frequency response of the plants in this region at every frequency. The general expression of a frequency domain region can e.g. be written as follows:

$$\mathcal{L} = \{G(z) \mid g(e^{j\omega}) \in U(\omega)\ \forall\omega\}, \tag{3.19}$$

where $g(e^{j\omega}) = \left(Re(G(e^{j\omega}))\ Im(G(e^{j\omega}))\right)^T$ and $U(\omega)$ is the particular domain where the frequency response vector of the plants $G(z) \in \mathcal{L}$ is constrained to lie at the frequency ω.

We are thus looking for the frequency domain region $\mathcal{L}$ that corresponds to the image of the set $\mathcal{D}$ in the Nyquist plane. Let us first define this notion properly.

Definition 2. Consider the set $\mathcal{D}$ of transfer functions defined in (3.7) and the general expression of a frequency domain region $\mathcal{L}$ given in (3.19). The image of $\mathcal{D}$ in the Nyquist plane is the frequency domain region $\mathcal{L}$ defined by (3.19) with $U(\omega)$ defined as follows, at each frequency ω:

$$U(\omega) = \{g(e^{j\omega}) \mid g(e^{j\omega}) = g(e^{j\omega}, \theta)\ \textit{for some}\ \theta \in U_\theta\} \tag{3.20}$$

with $g(e^{j\omega}, \theta)$ defined in (3.4). ■

Important comments. Definition 2 tells us

- that the image $\mathcal{L}$ of $\mathcal{D}$ in the Nyquist plane is a set containing the image of all plants in $\mathcal{D}$;
- that all "points $g(e^{j\omega}) \in U(\omega)$" at a frequency ω are the image of some plant in $\mathcal{D}$.

However, if we randomly select frequency functions $f(e^{j\omega}) \in \mathcal{L}$, for $\omega \in [0\ \pi]$, then most of such functions will not be in $\mathcal{D}$, i.e. for most of such functions $f(e^{j\omega}) \in \mathcal{L}$, there will not exist a θ such that $f(e^{j\omega}) = g(e^{j\omega}, \theta)\ \forall\omega$ with $g(e^{j\omega}, \theta)$ defined by (3.4).

Using the mapping (3.4) between the space of parametrized transfer functions $G(z, \theta)$ (or parameter space) and the frequency domain space, and the results of Theorem 1, we can construct an explicit expression of the image $\mathcal{L}$ of $\mathcal{D}$ in the Nyquist plane.

Theorem 3. *Consider the set $\mathcal{D}$ of transfer functions $G(z, \theta) = \bar{G}(z) + \Lambda(z)\theta$ presented in Definition 1, and the mapping (3.4) between parameter space and frequency domain space. The image of $\mathcal{D}$ in the Nyquist plane (see Definition 2) is a frequency domain region $\mathcal{L}$ having the following expression.*

$$\mathcal{L} = \{G(z) \mid g(e^{j\omega}) \in U(\omega)\ \forall\omega\} \tag{3.21}$$

$$U(\omega) = \{g \in \mathbf{R}^{2\times 1} \mid (g - \bar{g}(e^{j\omega}))^T P(\omega)^{-1}(g - \bar{g}(e^{j\omega})) < \chi\} \tag{3.22}$$

with $P(\omega) = T(e^{j\omega})P_\theta T(e^{j\omega})^T$,

$$g(e^{j\omega}) = \begin{pmatrix} Re(G(e^{j\omega})) \\ Im(G(e^{j\omega})) \end{pmatrix} \text{ and } \bar{g}(e^{j\omega}) = \begin{pmatrix} Re(\bar{G}(e^{j\omega})) \\ Im(\bar{G}(e^{j\omega})) \end{pmatrix}.$$

The image $\mathcal{L}$ of $\mathcal{D}$ in the Nyquist plane is thus made up of ellipses $U(\omega)$ at each frequency around the frequency response of the known transfer function $\bar{G}(z)$. The ellipse $U(\omega)$ at a particular frequency can therefore be considered as the image of $\mathcal{D}$ in the Nyquist plane at this frequency.

Proof. In order to establish the proof of Theorem 3, we need to prove that the expression (3.22) of $U(\omega)$ is equivalent with (3.20). The results follow directly from Theorem 1 by considering the mapping (3.4) (i.e. $g(e^{j\omega}, \theta) - \bar{g}(e^{j\omega}) = T(e^{j\omega})\theta$) at a particular frequency ω. ■

Remarks. It is to be noted that the matrix $P(\omega)$ defining $U(\omega)$ is equal to the covariance matrix $P_g(\omega)$ of $g(e^{j\omega}, \theta)$ (see (3.5)). It is also to be noted that, at the frequencies $\omega = 0$ and $\omega = \pi$, the ellipse $U(\omega)$ degenerates into a line segment.

3.5 Inverse image of $\mathcal{L}$

In the previous section, we have determined the frequency domain region $\mathcal{L}$, image of the set $\mathcal{D}$ of parametrized transfer functions $G(z,\theta)$. This set $\mathcal{L}$, made up of ellipses $U(\omega)$ at each frequency, is defined by the property (3.20). In particular, $\mathcal{L}$ contains all plants in $\mathcal{D}$. The set $\mathcal{L}$ is nevertheless not equivalent to $\mathcal{D}$. Indeed, we prove that there are more plants in $\mathcal{L}$ than those in $\mathcal{D}$. These additional plants are plants having a structure different from $G(z,\theta)$ (i.e. they cannot be described as $G(z,\theta)$ for any θ (see (3.1))), but also plants having the structure $G(z,\theta)$ but for $\theta \notin U_\theta$.

In this chapter, we will focus on the additional plants in $\mathcal{L}$ having the structure $G(z,\theta)$ given in (3.1) but for $\theta \notin U_\theta$. The fact that such additional plants exist in $\mathcal{L}$ is a consequence of the fact that the mapping (3.4) is not bijective[2] since (3.4) maps a k-dimensional space into the 2-dimensional frequency domain space. In order to establish that additional plants $G(z,\theta)$ lie in $\mathcal{L}$, the inverse image of $\mathcal{L}$ in the space of parametrized transfer functions $G(z,\theta)$ has to be determined. For this purpose, it is useful to first analyze the inverse image $\mathcal{D}(U(\omega))$, via the mapping (3.4), of one ellipse $U(\omega)$ of $\mathcal{L}$ in the space of parametrized transfer functions $G(z,\theta)$.

Proposition 1. *Consider a particular frequency ω and the ellipse $U(\omega)$ defined in (3.22) which is the image of the set $\mathcal{D}$ in the Nyquist plane at the frequency ω. Using the mapping (3.4) from θ to $g(e^{j\omega},\theta)$, define the inverse image of $U(\omega)$ in the parameter space as*

$$C_\theta(U(\omega)) = \{\theta \mid g(e^{j\omega},\theta) \in U(\omega)\}. \tag{3.23}$$

Correspondingly, define the inverse image of $U(\omega)$ in the space of parameterized transfer functions $G(z,\theta)$ as

$$\mathcal{D}(U(\omega)) = \{G(z,\theta) \mid g(e^{j\omega},\theta) \in U(\omega)\}. \tag{3.24}$$

Then the set $C_\theta(U(\omega))$ is a volume in the θ-space with $k-2$ infinite axes defined as:

$$C_\theta(U(\omega)) = \{\theta \in \mathbf{R}^{k\times 1} \mid \theta^T T(e^{j\omega})^T P(\omega)^{-1} T(e^{j\omega})\theta < \chi\}. \tag{3.25}$$

Moreover, $U_\theta \subset C_\theta(U(\omega))$ and $\mathcal{D} \subset \mathcal{D}(U(\omega))$.

Proof. The expression (3.25) of $C_\theta(U(\omega))$ follows directly from Theorem 2 by substituting $U(\omega)$ for U_x, U_θ for U_y and $C_\theta(U(\omega))$ for C_y. It then follows

[2] The mapping $T(e^{j\omega})$ is only bijective if the size k of the vector θ is equal to two.

from the last part of Theorem 2 that U_θ is a subset of $C_\theta(U(\omega))$. Now observe from (3.23) and (3.24) that $\mathcal{D}(U(\omega))$ can equivalently be described as

$$\mathcal{D}(U(\omega)) = \{G(z,\theta) \mid \theta \in C_\theta(U(\omega))\} \tag{3.26}$$

It then follows from $U_\theta \subset C_\theta(U(\omega))$ and the definitions (3.7) and (3.26) that $\mathcal{D} \subset \mathcal{D}(U(\omega))$. ■

Proposition 1 tells us that the ellipse $U(\omega)$ is the image of more plants $G(z,\theta)$ than those in $\mathcal{D}$. These additional plants $G(z,\theta_{out})$ with $\theta_{out} \in C_\theta(U(\omega)) \setminus U_\theta$, have the property that $\exists\, \theta_{in} \in U_\theta$ such that, *at frequency* ω,

$$g(e^{j\omega},\theta_{out}) = g(e^{j\omega},\theta_{in}),$$

since $U(\omega)$ is defined by (3.20).

It is also important to note that the inverse image $\mathcal{D}(U(\omega))$ of $U(\omega)$ in the space of parametrized transfer functions $G(z,\theta)$ is different at each frequency, because the inverse image $C_\theta(U(\omega))$ in parameter space is different at each frequency. In other words, $U(\omega)$ is the image of a set $\mathcal{D}(U(\omega))$ of plants $G(z,\theta)$ that are different at each frequency.

In Proposition 1, we have computed the inverse image $C_\theta(U(\omega))$ in parameter space of one ellipse $U(\omega)$, via the inverse of mapping (3.4). We now determine the inverse image $U_\theta(\mathcal{L})$ in parameter space of the whole set $\mathcal{L}$ defined by (3.21) and (3.22).

Theorem 4. *Consider the frequency domain set $\mathcal{L}$ defined by (3.21) and (3.22). Define the inverse image $U_\theta(\mathcal{L})$ of $\mathcal{L}$ in parameter space, via the mapping (3.4), as:*

$$U_\theta(\mathcal{L}) = \{\theta \mid G(z,\theta) \in \mathcal{L}\}. \tag{3.27}$$

Then

$$U_\theta(\mathcal{L}) = \bigcap_{\omega\in[0\ \pi]} C_\theta(U(\omega)), \tag{3.28}$$

where $C_\theta(U(\omega))$ is defined in (3.23) and (3.25). Moreover,

$$U_\theta \subseteq U_\theta(\mathcal{L}). \tag{3.29}$$

Proof. First observe that, by the definition of $\mathcal{L}$ in (3.21), the set $U_\theta(\mathcal{L})$ defined in (3.27) is equivalent with

$$U_\theta(\mathcal{L}) = \{\theta \mid g(e^{j\omega},\theta) \in U(\omega)\ \forall\omega\}.$$

The result (3.28) then follows immediately from Definition (3.23). The inclusion (3.29) then follows from the main result of Proposition 1, namely $U_\theta \subset C_\theta(U(\omega))\ \forall\omega$. ■

Corollary 1. *Consider the frequency domain set $\mathcal{L}$ defined by (3.21) and (3.22). Define the inverse image $\mathcal{D}(\mathcal{L})$ of $\mathcal{L}$ in the space of parametrized transfer functions $G(z,\theta)$, via the mapping (3.4), as*

$$\mathcal{D}(\mathcal{L}) = \{G(z,\theta) \mid G(z,\theta) \in \mathcal{L}\}. \tag{3.30}$$

Then $\mathcal{D} \subseteq \mathcal{D}_{\mathcal{L}}$.

Proof. By (3.30) and (3.27), it follows that

$$\mathcal{D}(\mathcal{L}) = \{G(z,\theta) \mid \theta \in U_\theta(\mathcal{L})\}. \tag{3.31}$$

The result then follows from the result (3.29) of Theorem 4, and the definition (3.7) of $\mathcal{D}$. ■

Corollary 2. *With definitions as above, we have:*

$$U_\theta \subseteq U_\theta(\mathcal{L}) \subset C_\theta(U(\omega)) \ \forall\omega \tag{3.32}$$

$$\mathcal{D} \subseteq \mathcal{D}(\mathcal{L}) \subset \mathcal{D}(U(\omega)) \ \forall\omega. \tag{3.33}$$

Proof. The first inclusions follow from Theorem 4 and Corollary 1. The second inclusion in (3.32) follows from (3.28), and the second inclusion of (3.33) from (3.31), (3.26) and (3.32). ■

Theorem 4 tells that the ellipsoid U_θ which defines $\mathcal{D}$ is a subset of $U_\theta(\mathcal{L}) = \bigcap_{\omega\in[0\ \pi]} C_\theta(U(\omega))$. We shall illustrate by an example in Section 8 that it may be a strictly proper subset of $U_\theta(\mathcal{L})$. As a consequence, $\mathcal{D}$ may be a strictly proper subset of $\mathcal{D}(\mathcal{L})$, and the frequency domain region $\mathcal{L}$ is therefore the image in the Nyquist plane of a set $\mathcal{D}(\mathcal{L})$ containing more plants $G(z,\theta)$ than those in $\mathcal{D}$. It is to be noted that, according to the definition of $\mathcal{L}$ (Definition 2), these additional plants $G(z,\theta_{out})$ with $\theta_{out} \in U_\theta(\mathcal{L}) \setminus U_\theta$, must have the property that, at each frequency ω, there exists θ_{in} in U_θ such that $G(e^{j\omega},\theta_{out}) = G(e^{j\omega},\theta_{in})$.

3.6 Probability level linked to the confidence region $\mathcal{L}$

In the previous sections, we have shown that the image of a set $\mathcal{D}$ in the Nyquist plane is a frequency domain region $\mathcal{L}$ made up of ellipses $U(\omega)$ at each frequency. We have also shown that the sets $U(\omega)$ and the whole region $\mathcal{L}$ are (or may be) the image of more plants $G(z,\theta)$ than those in $\mathcal{D}$. Let us

now consider both sets (i.e. $U(\omega)$ and $\mathcal{L}$) as confidence regions. The ellipse $U(\omega)$ is a confidence region for the frequency response vector $g(e^{j\omega},\theta)$ of the plants $G(z,\theta)$ and the set $\mathcal{L}$ is a confidence region for the plants $G(z,\theta)$. Since the parameter vector θ has a probability density function (see (3.2)), we can relate a probability level to both confidence regions.

Definition 3. Consider the parametrized transfer functions $G(z,\theta)$ given in (3.1), whose parameter vector θ has the probability density function (3.2). Consider also the sets $U(\omega)$ and $\mathcal{L}$ defined in (3.21)-(3.22). The probability level $\alpha(U(\omega))$ linked to $U(\omega)$ is defined as :

$$\alpha(U(\omega)) = Pr(g(e^{j\omega},\theta) \in U(\omega)),$$

where $g(e^{j\omega},\theta)$ is defined in (3.4). The probability level $\alpha(\mathcal{L})$ linked to $\mathcal{L}$ is defined as:

$$\alpha(\mathcal{L}) = Pr(G(z,\theta) \in \mathcal{L}).$$

■

These probability levels $\alpha(U(\omega))$ and $\alpha(\mathcal{L})$ will be larger than the probability level $\alpha(\mathcal{D})$ linked to $\mathcal{D}$ (i.e. $\alpha(\mathcal{D}) = 0.95$) since $\mathcal{D} \subseteq \mathcal{D}(\mathcal{L}) \subset \mathcal{D}(U(\omega))\ \forall\omega$ (see Corollary 2). Theorem 5 gives an exact computation of $\alpha(U(\omega))$, as well as upper and lower bounds for $\alpha(\mathcal{L})$.

Theorem 5. *Consider the parametrized transfer functions $G(z,\theta)$ given in (3.1), whose parameter vector θ has the probability density function (3.2). Consider also the sets $U(\omega)$ and $\mathcal{L}$ defined in (3.21)-(3.22). Then the probability level $\alpha(U(\omega))$ linked to $U(\omega)$ (see Definition 3) is given by:*

$$\alpha(U(\omega)) = Pr(G(z,\theta) \in \mathcal{D}(U(\omega))) \tag{3.34}$$

$$= Pr(\chi^2(2) < \chi)\ \forall\omega, \tag{3.35}$$

where $\mathcal{D}(U(\omega))$ is defined in (3.24). The probability level $\alpha(\mathcal{L})$ linked to $\mathcal{L}$ (see Definition 3) is bounded by:

$$\alpha(\mathcal{D}) \leq \alpha(\mathcal{L}) < \alpha(U(\omega)) \tag{3.36}$$

where $\alpha(\mathcal{D})$ is the probability level linked to the set $\mathcal{D}$ presented in Definition 1 and of which the set $\mathcal{L}$ is the image in the Nyquist plane ($\alpha(\mathcal{D}) = 0.95$).

Proof. That $\alpha(U(\omega))$ is equal to $Pr(G(z,\theta) \in \mathcal{D}(U(\omega)))$ follows from Proposition 1. That $\alpha(U(\omega))$ is also equal to (3.35) is a direct consequence of the probability density function of $g(e^{j\omega},\theta)$ given in (3.5) since the covariance matrix $P_g(\omega)$ of $g(e^{j\omega},\theta)$ is equal to the matrix $P(\omega)$ defining the ellipse $U(\omega)$.

Since the inverse image of $\mathcal{L}$ in the space of parametrized transfer functions $G(z,\theta)$ is $\mathcal{D}(\mathcal{L})$, we can write the following about the probability level $\alpha(\mathcal{L})$ linked to $\mathcal{L}$:

$$\alpha(\mathcal{L}) = Pr(G(z,\theta) \in \mathcal{D}(\mathcal{L})).$$

The upper bound in (3.36) proceeds then from the fact that $\mathcal{D}(\mathcal{L}) \subset \mathcal{D}(U(\omega))\ \forall\omega$ and the lower bound from the fact that $\mathcal{D} \subseteq \mathcal{D}(\mathcal{L})$ (see Theorem 4). ■

Important comments. Theorem 5 shows that the probability level $\alpha(\mathcal{L})$ linked to the image of $\mathcal{D}$ in the Nyquist plane is larger than the probability level linked to $\mathcal{D}$ (i.e. $\alpha(\mathcal{D}) = 0.95$). This is a consequence of the fact that $\mathcal{L}$ is the image of more plants than those in $\mathcal{D}$ because of the singularity of the mapping (3.4).

It is also interesting to note that if we consider the ellipses $U(\omega)$ frequency by frequency, these ellipses are the image in the Nyquist plane of a set $\mathcal{D}(U(\omega))$, different at each frequency, and having a probability level $\alpha(U(\omega))$ which follows from the probability density function (3.5) of $g(e^{j\omega},\theta)$. However, since the sets $\mathcal{D}(U(\omega))$ are different at each frequency, when we collect together all ellipses $U(\omega)$ to make up $\mathcal{L}$, the probability level $\alpha(\mathcal{L})$ is smaller than $\alpha(U(\omega))$. This last remark shows that the probability density function of $g(e^{j\omega},\theta)$ given in (3.5) is only relevant for one particular frequency. Theorem 5 shows therefore that, in order to design a confidence region $\mathcal{L}$ with a probability level $\alpha(\mathcal{L})$ larger than 95%, one has to first design a confidence region $\mathcal{D}$ having the desired probability level (i.e. $\alpha(\mathcal{D}) = 0.95$) and then take its image $\mathcal{L}$ in the Nyquist plane.

As a consequence, in the paper [7], the probability density function of the frequency response can be used in order to design a confidence ellipse of 95% *at a particular frequency*. However, these 95%-ellipses can not be connected in order to make up a frequency domain confidence region at 95% for the parametrized transfer functions, as proposed in [1,11]. For this purpose, as said above, one has to first design a confidence region $\mathcal{D}$ having the desired probability level (i.e. $\alpha(\mathcal{D}) = 0.95$) and then take its image $\mathcal{L}$ in the Nyquist plane, as proposed in [2].

Remarks. The plants having another structure than $G(z,\theta)$ and that lie in $\mathcal{L}$ do not modify the probability level $\alpha(\mathcal{L})$ since only the parameter vector θ has a probability density function.

3.7 Case of not linearly parametrized model structures

Until now, we have treated the case of systems $G(z,\theta)$ that can be written as in (3.1) and whose parameters have the probability density function (3.2). We have shown for this type of model structure the link between a set $\mathcal{D}$ of transfer functions $G(z,\theta)$ and its image $\mathcal{L}$ in the Nyquist plane. If the model structure is not linearly parametrized as in (3.1), our conclusions do not hold i.e. the image at a frequency ω is not guaranteed to be an ellipse. In [9,6,3], a first order approximation was used to map the parametric confidence ellipsoid into ellipses in the Nyquist plane. However, using such an approach, no probablity level can be guaranteed for the obtained frequency domain region.

As a consequence, it is very difficult to have a clear idea of the image in the Nyquist plane of a set $\mathcal{D}_{gen}$ of rational transfer functions with parameters appearing in both numerator and denominator. Some partial results have been presented in [4,5]. In [4], the authors have presented a way to compute, at each frequency, the largest and the smallest modulus and phase of the plants in a region $\mathcal{D}_{gen}$. In [5], we have given an LMI procedure that computes at each frequency the smallest overbounding ellipse that contains the frequency response of the plants in such set $\mathcal{D}_{gen}$.

3.8 Simulation example

In order to illustrate the results of this chapter, we present the following example. Let us consider the following system description:

$$\begin{aligned} G(z,\theta) &= \frac{0.08z^{-1}+0.1009z^{-2}+0.0359z^{-3}}{1-1.5578z^{-1}+0.5769z^{-2}} \\ &\quad + \frac{\theta_1 z^{-1}+\theta_2 z^{-2}+\theta_3 z^{-3}}{1-1.5578z^{-1}+0.5769z^{-2}} \\ &= \bar{G}(z) + \overbrace{\frac{1}{1-1.5578z^{-1}+0.5769z^{-2}}\begin{pmatrix} z^{-1} & z^{-2} & z^{-3}\end{pmatrix}}^{\Lambda(z)} \overbrace{\begin{pmatrix}\theta_1\\ \theta_2\\ \theta_2\end{pmatrix}}^{\theta} \end{aligned}$$

where the parameter vector θ is assumed to have a Gaussian probability density function with zero mean and covariance P_θ given by:

$$P_\theta = 10^{-3} \times \begin{pmatrix} 1.0031 & 0.0263 & -0.0111 \\ 0.0263 & 1.0039 & 0.0268 \\ -0.0111 & 0.0268 & 1.0039 \end{pmatrix}.$$

We consider the 95 % confidence ellipsoid U_θ in the parameter space that defines a corresponding region $\mathcal{D}$ in the space of transfer function:

$$U_\theta = \{\theta \mid \theta^T P_\theta^{-1} \theta < 7.81\},$$

$$\mathcal{D} = \{G(z,\theta) \mid \theta \in U_\theta\}$$

Using Theorem 3, we can design the image $\mathcal{L}$ of $\mathcal{D}$ in the Nyquist plane. This image $\mathcal{L}$ is made up of ellipses at each frequency around the frequency response of $\bar{G}(z)$ and is represented in Figure 3.1. According to Theorem 3, the expression of the ellipse $U(\omega)$ at the frequency ω is given by:

$$U(\omega) = \{g \in \mathbf{R}^{2\times 1} \mid (g - \bar{g}(e^{j\omega}))^T P(\omega)^{-1} (g - \bar{g}(e^{j\omega})) < 7.81\}$$

with $P(\omega) = T(e^{j\omega}) P_\theta T(e^{j\omega})^T$ and

$$\bar{g}(e^{j\omega}) = \begin{pmatrix} Re(\bar{G}(e^{j\omega})) \\ Im(\bar{G}(e^{j\omega})) \end{pmatrix}, \; T(e^{j\omega}) = \begin{pmatrix} Re(\Lambda(e^{j\omega})) \\ Im(\Lambda(e^{j\omega})) \end{pmatrix}.$$

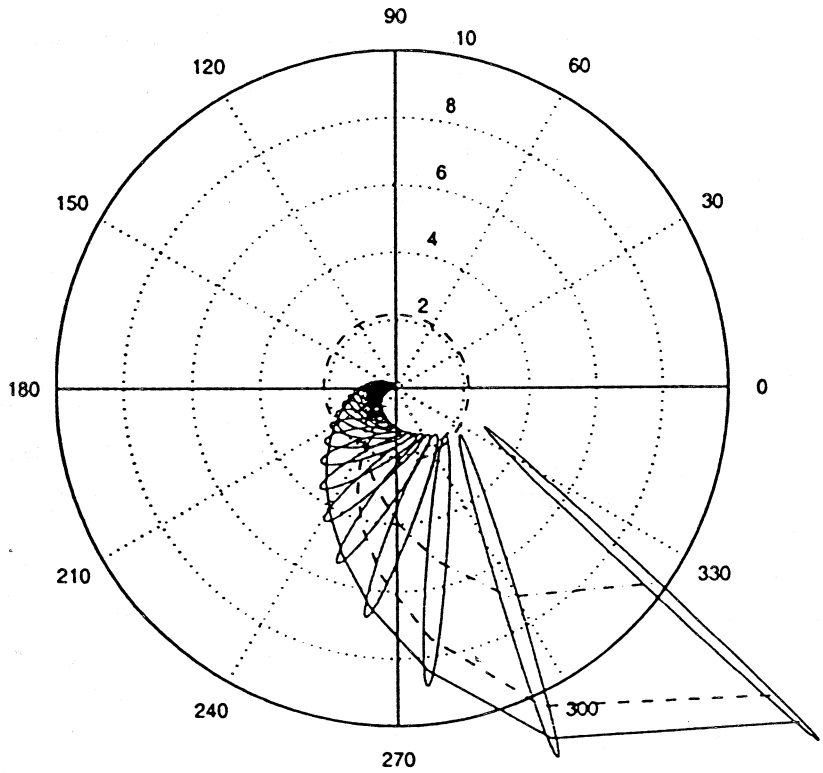

Fig. 3.1. Frequency domain representation of $\mathcal{D}$ in the Nyquist plane with ellipses $U(\omega)$ at some frequencies, frequency response of $\bar{G}(z)$ (dashdot), frequency response of $G(z,\theta_{out})$ (dashed) and frequency response of $G(z,\theta_{bis})$ (solid)

All plants in $\mathcal{D}$ lie in $\mathcal{L}$, and $\mathcal{L}$ has the property (3.20). However, the mappings between $\mathcal{D}$ and $\mathcal{L}$ and between $\mathcal{D}$ and $U(\omega)$ are not bijective as shown in Theorem 4 and Proposition 1, respectively. In order to illustrate the results presented in these theorems, we will show two things:

i. there exist plants $G(z,\theta_{out})$ outside $\mathcal{D}$ whose frequency response vector $g(e^{j\omega},\theta_{out})$ lies in some ellipses $U(\omega)$ but not in all of them;
ii. there exist plants $G(z,\theta_{bis})$ outside $\mathcal{D}$ that lie in the whole region $\mathcal{L}$.

Since the size of θ is 3, we know that the vectors θ that are projected into $U(\omega)$ at the frequency ω are those lying in the cylinder $C_\theta(U(\omega))$ whose axis direction is given by the normed eigenvector $\theta_{null}(\omega)$ corresponding to the null eigenvalue of the mapping $T(e^{j\omega})$ (see Theorem 2 and Proposition 1). Using this property, we can find a plant $G(z,\theta_{out})$ such that $\theta_{out} \notin U_\theta$, but such that its frequency response $g(e^{j\omega_0},\theta_{out})$ at ω_0 lies in $U(\omega_0)$ for a particular frequency ω_0, say $\omega_0 = 0.25$. Indeed, let us choose as vector θ_{out} a vector in the same direction as $\theta_{null}(0.25)$ but outside the ellipsoid U_θ:

$$\theta_{out} = \begin{pmatrix} 1.8084 \\ -3.5043 \\ 1.8084 \end{pmatrix}$$

This vector is well outside the ellipsoid U_θ since we have that:

$$\theta_{out}^T P_\theta^{-1} \theta_{out} = 19525 > 7.81$$

but we also have that:

$$g(e^{j0.25},\theta_{out}) = \bar{g}(e^{j0.25}) + \overbrace{T(e^{j0.25})\theta_{out}}^{=0} = \bar{g}(e^{j0.25}),$$

and therefore $g(e^{j0.25},\theta_{out})$ lies in $U(0.25)$. However, this plant does not lie in all ellipses as can be seen in Figure 3.1 where it circles around the origin at high frequencies.

There also exist plants $G(z,\theta_{bis})$ whose parameter vectors $\theta_{bis} \notin U_\theta$, but that lie completely in $\mathcal{L}$. According to Theorem 4 and Corollary 1, these are the plants whose parameter vectors θ_{bis} lie in $U_\theta(\mathcal{L}) = \bigcap_{\omega\in[0\ \pi]} C_\theta(U(\omega))$. In order to find one of those particular vectors θ_{bis}, we proceed like we did to find θ_{out}. We choose a particular frequency ω_0 and we choose a vector in the direction $\theta_{null}(\omega_0)$ of the axis of the cylinder $C_\theta(U(\omega_0))$. But, here, we choose this frequency ω_0 in the middle of the frequency range: $\omega_0 = \pi/2$ and we choose the vector **just** outside the ellipsoid U_θ:

$$\theta_{bis} = \begin{pmatrix} 0.0684 \\ 0 \\ 0.0684 \end{pmatrix}, \theta_{bis}^T P_\theta^{-1} \theta_{bis} = 9.4501 > 7.81.$$

In Figure 3.1, we see that the frequency response of the plant $G(z, \theta_{bis})$ lies in $U(\omega)$ for each of the plotted ellipses. Since we only plot the ellipses at a certain number of frequencies, Figure 3.1 alone does not prove that $G(z, \theta_{bis})$ is in $\mathcal{L}$. In Figure 3.2, we have therefore plotted the value of the function

$$(g(e^{j\omega}, \theta_{bis}) - \bar{g}(e^{j\omega}))^T P(\omega)^{-1} (g(e^{j\omega}, \theta_{bis}) - \bar{g}(e^{j\omega}))$$

at each frequency. We see that these values are, at each frequency, smaller than 7.81, the size of the ellipses $U(\omega)$. As a consequence, we can conclude that $G(z, \theta_{bis})$ has its frequency response in $\mathcal{L}$ even though $G(z, \theta_{bis})$ does not lie in $\mathcal{D}$.

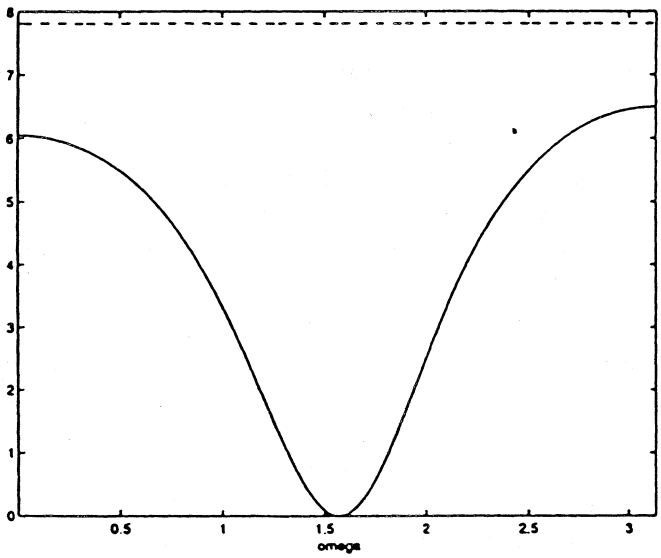

Fig. 3.2. Values of $(g(e^{j\omega}, \theta_{bis}) - \bar{g}(e^{j\omega}))^T P(\omega)^{-1} (g(e^{j\omega}, \theta_{bis}) - \bar{g}(e^{j\omega}))$ as a function of the frequency (solid) and size of the ellipses $U(\omega)$ (dashed)

3.9 Conclusions

In this chapter, we have considered linearly parametrized plants $G(z, \theta)$ whose parameters are normally distributed and we have presented results about the image $\mathcal{L}$ in the Nyquist plane of a confidence region $\mathcal{D}$ in the space of parametrized transfer functions. We have shown that this image is made of ellipses at each frequency. However, since the mapping between these two

spaces is not bijective, the image $\mathcal{L}$ in the Nyquist plane contains more plants $G(z,\theta)$ than the initial confidence region $\mathcal{D}$. The image in the Nyquist plane is thus also a confidence region for the parametrized plants $G(z,\theta)$ but with a probability level larger than that of the initial confidence region $\mathcal{D}$.

Acknowledgments

We would like to thank Glenn Vinnicombe, Paresh Date and John Steele of the University of Cambridge who have motivated us to analyze this problem.

References

1. P. Andersen, S. Toffner-Clausen, and T.S. Pedersen. Estimation of frequency domain model uncertainties with application to robust control design. In *Proc. IFAC Symposium on System Identification*, pages 603–608, Copenhagen, 1994.
2. X. Bombois, M. Gevers, and G. Scorletti. Controller validation for stability and performance based on a frequency domain uncertainty region obtained by stochastic embedding. Accepted for presentation at CDC 2000, Sydney, Australia.
3. X. Bombois, M. Gevers, and G. Scorletti. Controller validation for a validated model set. In *CD-ROM Proc. European Control Conference*, paper 869, Karlsruhe, Germany, 1999.
4. G. Chesi, A. Garulli, A. Tesi, and A. Vicino. Exact bounds for the frequency response of an uncertain plant with ellipsoidal perturbations. In *CD-ROM Proc. IFAC Symposium on System Identification*, paper WeMD1-5, Santa Barbara, California, 2000.
5. M. Gevers, X. Bombois, B. Codrons, F. De Bruyne, and G. Scorletti. The role of experimental conditions in model validation for control. In A. Garulli, A. Tesi, and A. Vicino, editors, *Robustness in Identification and Control - Proc. of Siena Workshop, July 1998*, volume 245 of *Lecture Notes in Control and Information Sciences*, pages 72–86. Springer Verlag, 1999.
6. M. Gevers, B. Codrons, and F. De Bruyne. Model validation in closed-loop. In *Proc. American Control Conference,*, pages 326–330, San Diego, California,1999.
7. G.C. Goodwin, M. Gevers, and B. Ninness. Quantifying the error in estimated transfer functions with application to model order selection. *IEEE Trans. Automatic Control*, 37:913–928, 1992.
8. G.C. Goodwin, L. Wang, and D. Miller. Bias-variance trade-off issues in robust controller design using statistical confidence bounds. In *Proc. IFAC World Congress*, Beijing, 1999.
9. L. Ljung. Identification for control - what is there to learn? *Workshop on Learning, Control and Hybrid Systems, Bangalore*, 1998.
10. L. Ljung. Model error modeling and control design. In *CD-ROM Proc. IFAC Symposium on system identification*, paper WeAM1-3, Santa Barbara, California, 2000.
11. S. Toffner-Clausen, P. Andersen, J. Stoustrup, and H.H. Niemann. Estimated frequency domain model uncertainties used in robust controller design - a μ-approach. In *Proc. IEEE Conference on Control Applications*, pages 1585–1590, Glasgow, 1994.

12. L. Wang, G.C. Goodwin, and D.H. Owens. Robust controller design for unstable systems using statistical confidence bounds. In *Proc. European Control Conference*, Karlsruhe, 1999.
13. K. Zhou, J.C. Doyle, and K. Glover. *Robust and Optimal Control.* Prentice Hall, New Jersey, 1995.